Journal of Molecular Catalysis A: Chemical 315 (2010) 28–34

Contents lists available at ScienceDirect

Journal of Molecular Catalysis A: Chemical

journal homepage: www.elsevier.com/locate/molcata

Theoretical study of Au/SAPO-11 catalyst and its potential use in thiophene HDS

Beulah Griffe[a,*], Joaquín L. Brito[a], Anibal Sierraalta[b]

[a] Laboratorio de Físico-química de Superficies, Centro de Química, Instituto Venezolano de Investigaciones Científicas, I.V.I.C., Apartado 20632, Caracas 1020-A, Venezuela
[b] Laboratorio de Química Computacional, Centro de Química, Instituto Venezolano de Investigaciones Científicas, I.V.I.C., Apartado 20632, Caracas 1020-A, Venezuela

ARTICLE INFO

Article history:
Received 6 April 2009
Received in revised form 4 August 2009
Accepted 13 August 2009
Available online 22 August 2009

Keywords:
ONIOM
Computational catalysis
Au/SAPO-11
Theoretical calculations
Thiophene HDS

ABSTRACT

Quantum chemistry calculations were carried out, using ONIOM2 methodology, in order to investigate the thiophene interaction with gold supported on silicoaluminophospates molecular sieves (Au/SAPO-11) catalysts. Two models were studied, one containing one Au atom per site, and the other with two Au atoms per site. Thiophene adsorption was found to be η^1 type. This adsorption presents a ΔH of −13.2 and −9.7 kcal/mol, for the models with one Au atom (Au/SAPO-11), and two Au atoms (Au_2/SAPO-11), respectively. The partial hydrogenation of the thiophene–Au/SAPO-11 and thiophene–Au_2/SAPO-11 complexes gives 2,5-dihydrothiophene (DHT), with a ΔH of −23.0 and −36.8 kcal/mol, respectively. 2-Butene production was found in both models with further hydrogenation. Likewise the direct butadiene elimination is achieved, but only with the separated Au dimer ($\Delta H = -17.5$ kcal/mol).

1. Introduction

For a long time, gold was only occasionally mentioned in the literature with respect to its use as catalyst. This was due to its inability to chemisorb small molecules at low temperatures which makes it function as poor catalysts. Besides its inertness, Au is a metal difficult to be dispersed on supports. However, in 1987 Haruta et al. [1] reported that the Au could be a good catalyst, and showed that the catalytic behavior of gold depends markedly on the dispersion, the support and the preparation method. When gold is deposited on selected metal oxides as hemispherical ultra-fine particles with diameters smaller than 5 nm, it exhibits surprisingly high activity and/or selectivity in CO and saturated hydrocarbons combustion; amines and organic halogenated compounds oxidation–decomposition; hydrocarbons partial oxidation; the hydrogenation of carbon oxides, unsaturated carbonyl compounds, alkynes and dienes; and the reduction of nitrogen oxides [1,2]. Recently, Au has attracted much attention, not only in heterogeneous catalysis, but in colloidal chemistry and nanocomponents manufacture, and some other applications [3].

Zeolites have been considered as very interesting host materials to disperse Au, due to their pores internal distribution and the possibility of controlling the particle size [3–5]. Intrazeolitic Au catalysts have been investigated in various reactions such as water gas shift reaction and NO reduction by CO in the absence and presence of hydrogen [5–8]. NO reduction with H_2 [9], and with propene [10] was also reported. Haruta et al. [11–14] published several articles in propene oxidation to propylene oxide over highly dispersed nanosize Au particles supported on titanosilicates such as TS-1, Ti-MCM-41 and Ti-MCM-48.

Silicoaluminophospates (SAPO) molecular sieves have been considered attractive materials to be used in heterogeneous catalysis either as catalysts themselves or as supports. For instance, SAPO-11 is used as a catalyst in the methanol conversion reaction to hydrocarbons. The formation of higher carbon number products on SAPO-11 on this reaction is caused by the lower reactivity of the active centers for cracking reactions [15]. In the methanol dehydration and direct dimethylether production from synthesis gas, SAPO-5 and SAPO-11 showed relatively high catalytic stability. The high stability of these catalysts is endorsed to their mild acid sites and desirable pore architecture [16]. The skeletal isomerization of 1-pentene was investigated over SAPO-11 and other molecular sieves and the acidity of the catalysts seems to play a more important role than the pore size in the reaction conditions used [17]. SAPO-11 synthesized from non-aqueous medium, showed higher conversions and higher selectivity for acid-catalyzed m-xylene isomerization reaction than the SAPOs synthesized from aqueous media [18]. On the other hand, the use of metals supported on SAPO-11, such as Pt/SAPO-11, has been reported in *n*-alkane isomerization with high activity and selectivity, due to their unique combination of mild acidity and shape selectivity [19–23]. Pd/SAPO-11 was studied in n-heptane hydroisomerization [24] and Ga/SAPO-11 catalyst has been used in the direct transformation of *n*-butane to *iso*-butane [25,26].

* Corresponding author. Tel.: +58 212 5041828; fax: +58 212 5041350.
E-mail address: bgriffe@ivic.ve (B. Griffe).

1381-1169/$ – see front matter © 2009 Elsevier B.V. All rights reserved.
doi:10.1016/j.molcata.2009.08.010

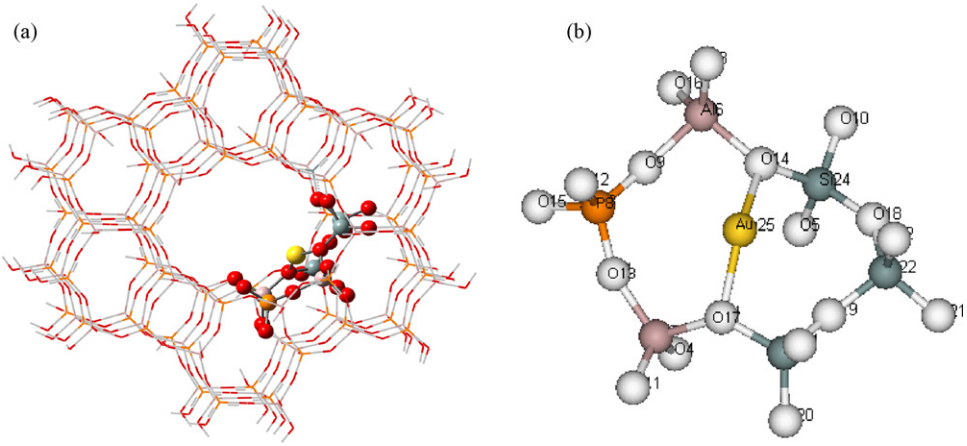

Fig. 1. (a) Molecular structure used to represent Au/SAPO-11, with the two levels of calculation, high level highlighted with spheres and low level represented with sticks. (b) Close view of T6 showing Au interacting with two oxygens in the structure (25 atoms).

As mentioned above, numerous reactions have been studied using Au supported on different zeolites [3–14]. SAPO-11 has been reported as an interesting material itself and as support in several catalytic reactions [15–26], nevertheless, only one publication was encountered on Au/SAPO-18, over a series of mesoporous and microporous materials containing gold nano-particles to investigate the effects of the host matrix and preparation methods on the properties of gold nano-particles [27]. SAPO-11 has proved to have stability in various reactions, endorsed to mild acid sites and desirable pore architecture, thus, we consider interesting to investigate the system Au/SAPO-11. In this work, we present a quantum chemical study, using the ONIOM2 method, on gold supported on silicoaluminophospates, SAPO-11, for thiophene hydrodesulfurization (HDS).

2. Computational details and models

All geometry optimizations and energy calculations were performed using the Gaussian-03 program [28]. The lower energy structures were obtained using the two-layer ONIOM2 methodology. For the high level, (represented by spheres in Fig. 1), DFT approach (B3LYP) with the full-electron 3-21G* basis set for H, C and O and LANL2DZ with its pseudo potentials for the rest of atoms of the SAPO-11 ring, Si, Al, P, composed by 6 tetrahedral was employed. All adsorbed and reactive molecules were included in the high level.

Universal force field approach (UFF) was employed for the low level (represented by sticks in Fig. 1). H atoms were used as boundary atoms in the ONIOM2 calculations.

The silicoaluminophospates molecular sieves (SAPO) are molecular structures that contain Si–O–Al, P–O–Al and Si–O–Si but no Si–O–P bonds (see Fig. 1). They have a medium size pore structure with low density of moderate acid sites. The SAPO-11 principal channel contains rings of 10 tetrahedrons (T10). The Brönsted acid sites of these structures are protons attached to the oxygen bridge of the Si–O–Al triads; mainly, inside the T10 rings. To model the SAPO-11, we used a cluster model with a four layer structure, where each layer contains a T10 ring (4T10). This model comprises a total of 506 atoms and was already described in a previous work [29].

The bond indexes (BI) were calculated using Wiberg Bond Indexes in the NAO Basis (Natural Atomic Orbital) approximation. Net charges reported are Mulliken atomic charges.

Thermodynamic properties were calculated at 298.15 K, using only the high level model.

Generally, the quality of the results using ONIOM is similar to those computed with periodical calculations [29,30] and with less computational cost, than did with comparable constrained clusters [31]. Moreover, it has been shown in the literature that the computed adsorption energies with ONIOM method compared well with experimental results [32–35].

3. Results and discussion

3.1. Au/SAPO-11 and Au_2/SAPO-11 models

Fig. 1a displays the molecular structure of Au/SAPO-11 model showing the two levels of calculation and (b) shows a detail of the high level 25 atoms $AuAl_2Si_3PO_{18}$ of the model. In this model the gold formal oxidation state is 1+. This and the 3+ state are the most common Au oxidation states. Sachtler and co-workers [36] as well as Ichikawa and co-workers [8,37,38] have published that one of the gold species present on Au/MFI catalyst is Au^{1+}. In MgO-supported catalyst, the gold is present as cationic and zerovalent. The catalytic activity increases with an increasing of the fraction of cationic gold [39]. Alternatively other oxidation states are possible and they cannot be ruled out. For example, Roduner and co-workers [4] using electron spin resonance (ESR), reported the existence of Au^{2+} which could be stabilized by the Y supercage zeolite. Pestryakov et al. [40,41] analyzing the preparation of Au-zeolites, identified the Au^{3+} state, *partly reduced species* with charge $Au_n^{\delta+}$, and Au^0 nano-particles with diameter within interval of 1.5–20 nm. The authors suggested that all these species can be stabilized inside zeolite channels.

Table 1 shows the geometrical properties of Au supported on SAPO-11 model (Fig. 1a). According to the results, the Au minimum energy geometry corresponds to a position where the Au atom interacts with two SAPO-11 T6 ring oxygen atoms (see Fig. 1b). The Au atom is localized at equidistant distances of both oxygen atoms, 2.08 and 2.09 Å, respectively. The bond indexes (BI) and the net charge were also calculated and revealed that the Au net charge is close to unity, (Q_{Au} = +0.71e), that means that the Au formal oxidation state is 1+. The BI shows that Au share bonds mainly, with O14 and O17 (Total B = 0.52) and some other atoms in the surface (see Fig. 2). To know how strong the Au atom is bonded to the SAPO-11 structure, it is necessary to calculate the bonding energy. To estimate this bonding energy or the enthalpy, we choose the dissociation reaction (1) as a reference. The Au binding ΔH (ΔH = −71.9 kcal/mol) calculated according to reaction (1), reveals that the gold atom is strongly bonded to structure

$$\text{Au/SAPO-11} \rightarrow [\text{SAPO-11}] + \text{Au}^{(0)} \quad (1)$$

Table 1
Relevant bond distances (R) and bond angles of SAPO-11, Au/SAPO-11 and Au_2/SAPO-11, thiophene(Th)–Au/SAPO-11 and thiophene(Th)–Au_2/SAPO-11. Values corresponding to Au_2/SAPO-11 are in parentheses.

Bond/angle	SAPO-11	Au/SAPO-11(Au_2)	Th–Au/SAPO11(Au_2)
R O14–Si	1.61 Å	1.65 Å (1.64)	1.63 Å (1.60)
Si–O14–Al	150.6°	133.3° (137.8)	133.9° (151.1)
R O14–Al	1.68 Å	1.79 Å (1.74)	1.74 Å (1.69)
R O17–Si	1.65 Å	1.66 Å (1.65)	1.66 Å (1.66)
Si–O17–Al	140.6	131.9° (136.5)	132.0° (137.5)
R O17–Al	1.74 Å	1.78 Å (1.80)	1.78 Å (1.80)
Au–S			2.43 Å (2.44)
Au–Au		(2.98 Å)	(3.12 Å)
Au–O14		2.08 Å (2.36)	3.24 Å (3.17)
Au–O17		2.09 Å (2.29)	2.09 Å (2.17)
O14–Au–O17		146.6° (110.3)	91.6° (97.2)
RO1–Si		(1.68 Å)	(1.67 Å)
Si–O1–Al		(131.1°)	(137.1°)
RO1–Al		(1.80 Å)	(1.79 Å)
RO33–Si		(1.65 Å)	(1.65 Å)
Si–O33–Al		(131.4°)	(138.1°)
RO33–Al		(1.79 Å)	(1.77 Å)
Au–O1		(2.09 Å)	(2.06 Å)
Au–O33		(2.11 Å)	(2.07 Å)
O1–Au–O33		(144.8°)	(164.5°)

The Au binding ΔH is defined as $\Delta H = H_{Au/SAPO\text{-}11} - (H_{[SAPO\text{-}11]} + H_{Au})$ where ΔH is the binding enthalpy or adsorption enthalpy; and $H_{Au/SAPO\text{-}11}$, $H_{[SAPO\text{-}11]}$, and H_{Au} are the enthalpies of the aggregate Au/SAPO-11, the neutral support SAPO-11 without the hydrogen of the acid Brönsted site, and the atomic Au.

It has been reported experimentally, that the Au^{3+} species present in the supported gold catalyst, can be reduced to Au^+ by CO [8,38,39]. In order to investigate this possibility, quantum calculations were performed for the reaction of Au^{3+} reduction in agreement with reaction (2a). The Au^{3+} species was modeled by the $[OAu]^+$ moiety.

$$OAu/SAPO\text{-}11 + CO \rightarrow Au/SAPO\text{-}11 + CO_2 \quad (2a)$$

In the OAu/SAPO cluster the $[OAu]^+$ moiety is localized between two T6 ring oxygens at 2.04 and 2.05 Å, respectively, as shown in Fig. 3. These distances are shorter than the corresponding to the Au^+. The total bond indexes (BI = 0.60) indicate that the $[OAu]^+$ moiety is bonded to the SAPO-11 structure in a similar way to Au^+. The $[OAu]^+$ net charge is +1.36 therefore, the formal Au charge is 3+. The enthalpy change ΔH for reaction (2a) (−108.6 kcal/mol) reveals that reaction (2a) is highly exothermic consequently, the Au^{3+} species can be reduced by CO. In order to estimate the influence of the support on the reduction of the AuO supported species,

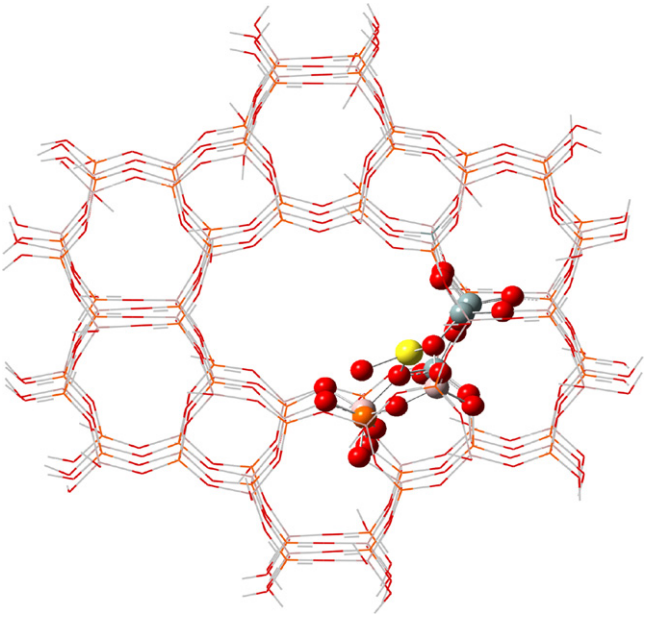

Fig. 3. OAu/SAPO-11, showing the $[OAu]^+$ moiety, see reaction (2a).

we performed enthalpy calculations for the following reactions in gas phase:

$$AuO^{(0)} + CO = CO_2 + Au^{(0)} \quad \Delta H = -73.0\,kcal/mol \quad (2b)$$

$$AuO^+ + CO = CO_2 + Au^+ \quad \Delta H = -135.5\,kcal/mol \quad (2c)$$

The enthalpy values for reactions (2b) and (2c) show that the ΔH value for reaction (2a) is between both values and close to the corresponding values of reaction (2c). Considering that the net charge of the $[OAu]^+$ moiety in the OAu/SAPO-11 models has a formal charge quite close to 1+, the difference between the enthalpy values for reactions (2c) and (2a) could be attributed to the support effect, that stabilize the $[OAu]^+$ moiety as well as the Au^+. Consequently, this suggests that if the Au^+ is the active site, the catalytic activity of Au/SAPO-11 catalyst can be increased by a pre-treatment with CO.

Some authors [40,41] have suggested that besides the Au^+ and Au^{3+} species, some kind of $Au_n^{\delta+}$ clusters can be present in gold catalysts. The SAPO-11 internal structure and atom distribution types are such that allows having two near Brønsted acid sites. In this situation it is possible to have two gold atoms closed enough that could be considered as an $Au_2^{\delta+}$ cluster. To study this possibility, quan-

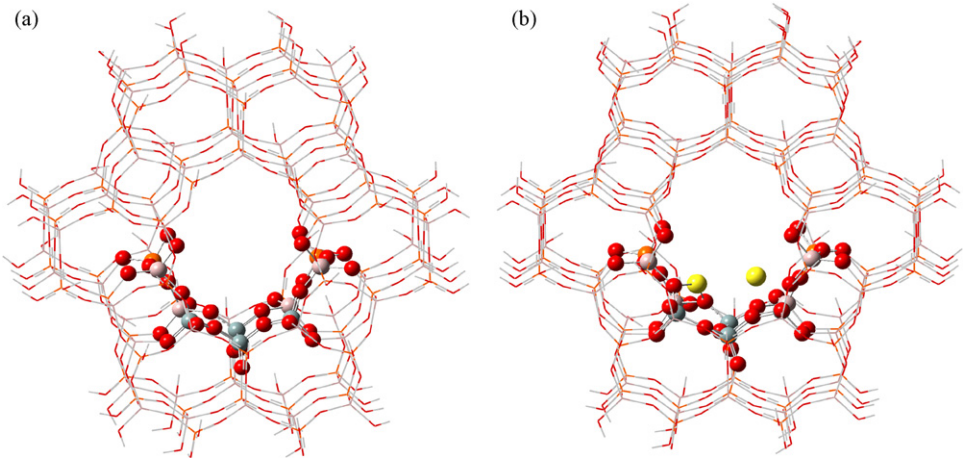

Fig. 2. (a) SAPO-11 structure employing a larger high level model (39 atoms). (b) Two gold atoms interacting with the structure 2a.

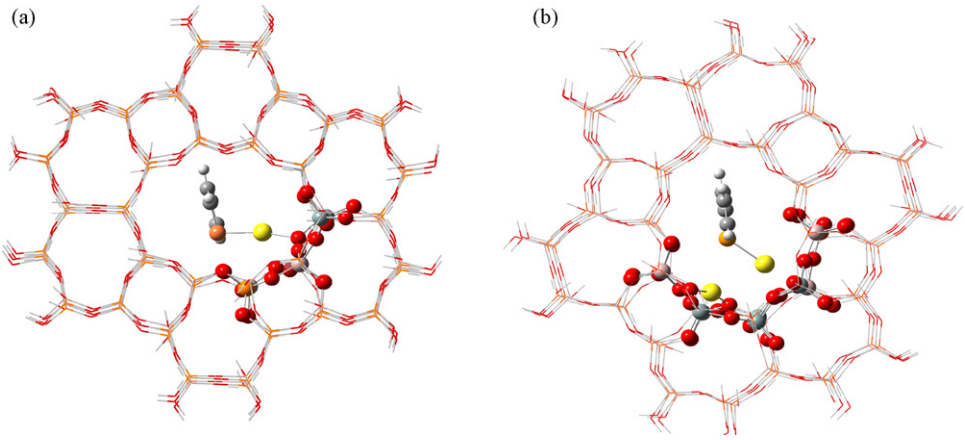

Fig. 4. Thiophene interaction with: (a) Au/SAPO-11 and (b) Au_2/SAPO-11.

tum chemical calculations were performed on Au_2/SAPO-11 model. To have two gold atoms inside the SAPO-11 cavity, it is necessary to increase the size of the high level. Fig. 2 shows the new SAPO-11 model (Fig. 2a). The Au_2/SAPO-11 minimum enthalpy structure $\Delta H = -111.5$ kcal/mol is set in Fig. 2b. ΔH was calculated according to reaction (3)

$$Au_2/SAPO\text{-}11 \rightarrow [SAPO\text{-}11] + Au_2^{(0)} \quad (3)$$

Table 1 points up that in the Au_2/SAPO-11 cluster one of the Au (Au1) is bonded to two oxygen atoms, O1 and O33 at 2.09 and 2.11 Å respectively, and to other one (Au2), to the O17 at 2.29 and to O14 at 2.36 Å. The Au1 bond indexes are 0.30 and 0.23, whereas for the Au weakly bonded, Au2, the bond indexes are 0.12 and 0.16, confirming that there is an Au stronger bonded than the other one. The Au1 and Au2 net charges are +0.77e and +0.69e. The high Au net charges [42] and the relative low Au BI indicate that the Au-support interaction has an important electrostatic component higher than the covalent interaction. On the other hand, the Au–Au BI = 0.12 as well as the Au–Au distance, 2.98 Å, show that there is an inter-metallic interaction between both Au atoms. This Au_2 moiety geometry does not correspond to a ground state Au_2 dimer. Calculation for Au_2 dimer in gas phase show that the Au–Au distance is 2.57 Å and the BI = 1.0.

3.2. Thiophene adsorption on –Au/ and –Au_2/SAPO-11

Contradictory reports have been published in the literature regarding the interaction between thiophene (Th) and gold. Earlier works, both experimental [43] and theoretical [44] suggested that the gold surface does not react with thiophene. On the other hand, several studies have shown the opposite, the strong affinity of gold for sulfur compounds [45–47]. Recently, it has been shown that self-assembled monolayers result from the strong interaction of Au with thiophene adsorbed from solutions [48–53] and thiophene adsorbed from the gas phase under reduced pressures weakly chemisorbs on the gold surface [54,56]. Moreover, this affinity of gold with sulfur compounds is exploited in gas sensors for the detection of H_2S and in molecular electronics devices [2,56]. Since the gold atoms in the Au/SAPO-11 catalyst are located inside the pores, it is reasonable to expect that the thiophene molecule be forced to interact with the Au atoms. In order to investigate this possibility quantum chemical calculations were performed on thiophene–Au and thiophene–Au_2/SAPO-11 systems.

Calculations show that there are several low energy conformations. The most stable conformations are η^1-type adsorption modes (trough the electron pair of S) as displayed in Fig. 4 for both Au and Au_2/SAPO-11. This adsorption mode is similar to the reported in the literature for Mo case [57]. In Fig. 4b it can be observed that in Au_2/SAPO-11, the thiophene adsorption takes place on the Au weakly bonded to the substrate. The calculated thiophene adsorption enthalpy change for Au/ and Au_2/SAPO-11 systems are $\Delta H = -13.2$ and -9.5 kcal/mol respectively. The calculations show that the thiophene adsorption enthalpy in Au/ and Au_2/SAPO-11 are similar. As long as the adsorption ΔH is a relevant parameter for describing the Th–Au interaction, our results seem to indicate that the thiophene interacts with only one Au atom in Au_2/SAPO-11, as in the Au/SAPO-11 case.

These adsorption enthalpy values are relatively low compared to the thiolate molecules adsorption energy values, which are in the range -23.5 to -37.1 kcal/mol [47]. In order to estimate if the adsorption enthalpy values of -13 to -10 kcal/mol are reasonable, we calculated the adsorption enthalpy of methyl thiolate on Au/SAPO-11. The result, -28.7 kcal/mol, is in the range for the thiolate molecules adsorption energies. Therefore, the values of $\Delta H = -13.2$ and -9.5 kcal/mol are coherent. Besides, these results could be supported by the Th desorption energies reported [54,55,58]. Liu et al. [54] described three estimated desorption energies, 18, 16 and 11 kcal/mol. These desorption energies were obtained for different amount of thiophene exposures. Nambu et al. [55] published that the desorption energies are 13 and 11 kcal/mol for flat and compressed monolayer of thiophene adsorption on Au.

These values indicate that thiophene could adsorb on Au/SAPO-11 catalysts at room temperature. The SAPO-11 cavity constrains the thiophene molecule helping the processes of the thiophene adsorption on gold.

Comparing some bond distances (R) and bond angles (BA) in thiophene–Au/ and thiophene–Au_2/SAPO-11 systems (see Table 1), it can be observed that one of Au–O bonds (Au–O14) is broken or enlarged, due to the Au interaction with thiophene. In the case of thiophene–Au/SAPO-11, the distance R Au–O14 increases from 2.08 to 3.24 Å and in the case of thiophene–Au_2/SAPO-11, the same bond increases from 2.36 to 3.17 Å. Whereas, BA contracts (tightens) from 146.6° to 91.6° in thiophene–Au/SAPO-11 and from 110.3° to 97.2° in Au_2/SAPO-11. The distance Au–Au increases after the thiophene interaction from 2.98 to 3.12 Å. The rest of substrate geometrical properties remained almost unaffected.

The C–S bond distance in thiophene–Au/SAPO-11 is 1.82 Å and in thiophene–Au_2/SAPO-11, one bond is at 1.81 Å, whereas in free thiophene is 1.79 Å. This fact seems to indicate a small activation of C–S bond. The bond indexes (BI) and the net charges revealed that in both cases: Au and Au_2/SAPO-11, the thiophene molecule is adsorbed with charge transference from it to the Au. Thus, Au charge is +0.70 before thiophene adsorption and +0.60 after the adsorption. Whereas in Au_2/SAPO-11 the Au1 and Au2 net charges are +0.77 and +0.69 before thiophene adsorption and +0.65 and

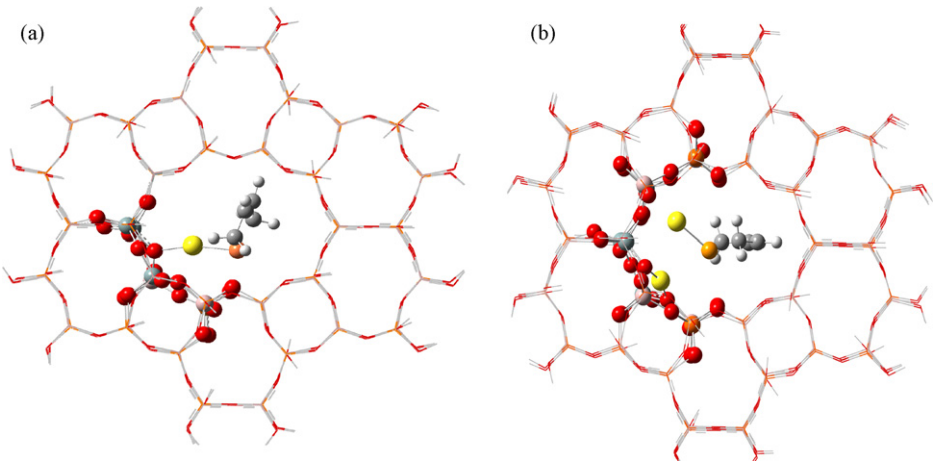

Fig. 5. 2,5-DHT obtained by hydrogenation of thiophene: (a) on Au/SAPO-11 and (b) on Au_2/SAPO-11.

+0.66 after the adsorption. The charge analysis shows that the charge transfer comes from the thiophene C atoms. They are slightly oxidized while the Au is reduced. C–S BI changes from 1.17 in free thiophene to 1.04 and 1.07 in thiophene–Au/SAPO-11 and thiophene–Au_2/SAPO-11. These facts point to an activation process of the bonds due to the adsorption.

3.3. *Modeling of HDS reaction of thiophene–Au/ and –Au_2/SAPO-11*

In a published theoretical study by Yao et al. [59] about the reaction mechanism of thiophene hydrodesulfurization (HDS) on a Mo3S9 model catalyst, the authors identified the 2,5-dihydrothiophene (DHT) molecule as the most important intermediate of HDS processes, and responsible for the direct formation of butadiene as the principal product. The butadiene molecule is obtained by direct intramolecular elimination of sulfur from 2,5-DHT. Butane and cis-butene could also be obtained but with larger activation energies through stepwise hydrogenation of 2,5-DHT or either from hydrogenation or the formed butadiene.

Sullivan and Ekerdt [57] proposed a similar mechanism for thiophene HDS on silica-supported molybdenum catalysts. The major path for HDS of thiophene is the elimination of sulfur from 2,5-DHT to produce butadiene. 1-Butene, 2-butene, and *n*-butane are formed by hydrogenation and isomerization. Prins et al. [60], published that on deep HDS of 4,6-dimethyldibenzothiophene using Pd catalyst, the de-hydrogenation reactions were relatively fast compared to the C–S bond breaking reactions, whereas the reverse was true over the metal sulfide catalyst. Saintigny et al. [61] proposed an alternative mechanism. This mechanism corresponds to the thiophene cycle opening and the consecutive formation of thiols derivatives as intermediates. These authors used, however acid zeolites [61].

Concerted mechanisms were used to explain the heterogeneous catalysis by sulfides [62] in which, there is a synchronous interaction of the reactive molecules in the coordination sphere of the bimetallic active centers (proton and electron transfer), involving the electronic structure of metals, the sulfide component, the dihydrogen. In this sense, catalytic transformations over the sulfide HDS catalysts are considered to belong to the acid–base catalysis.

Recently Joshi et al. [63] published a theoretical investigation of the active phase-support interaction for HDS catalysts using DFT to calculate the thiolysis and hydrolysis reaction energies for the metal support linkages. These metal-support bonds are represented by simplified cluster models simulating thiolysis and hydrolysis reactions. The calculated rank order of the metal oxide supports Type I (strong interaction) agrees with the experimentally observed.

Hinnemann et al. [64] highlighted some recent density functional theory (DFT) studies of hydrodesulfurization (HDS) of both un-promoted MoS_2 and promoted Co–Mo–S and Ni–Mo–S nanostructures. They give a picture not only of the structure of the active phase but on the reaction path way for thiophene HDS. The calculations provided a detailed picture of the reaction network of thiophene HDS on MoS_2. One important result is that the HDS reac-

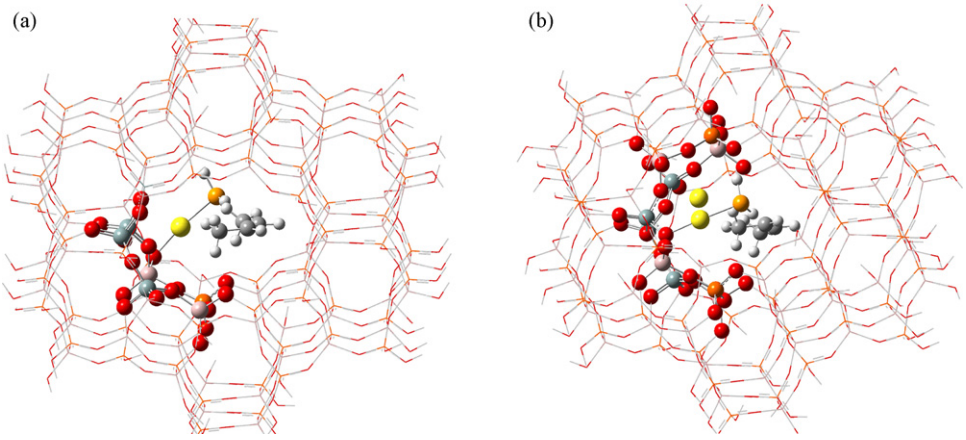

Fig. 6. Thiophene HDS to 2-butene: (a) Au/SAPO-11 and (b) Au_2/SAPO-11 with separated Au atoms (thiophene + $3H_2$).

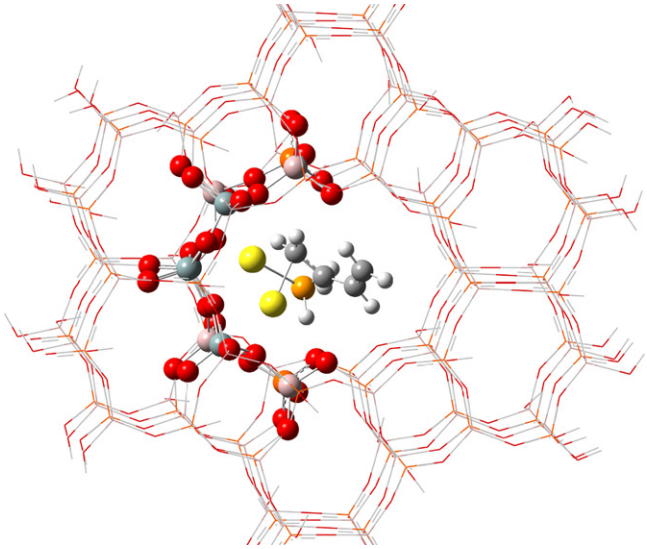

Fig. 7. Thiophene HDS to butadiene, via 2,5-dihydrothiophene on Au_2/SAPO-11 (thiophene + $2H_2$).

tion uses different active sites depending on the specific reaction conditions, and that the reaction is a complex interplay between Mo-edge brim sites and S-edge vacancy sites. The calculations revealed that the hydrogenation steps in the hydrogenation (HYD) pathway should preferably take place at the Mo edge. However, all S–C bond scission steps, i.e. the final S–C scission step in the HYD pathway and S–C scission in the direct desulfurization (DDS) pathway, seem to be more facile at the S edge, and therefore they probably take place there. Also a combination of theoretical and experimental results was published to support these mechanisms [65,66].

In order to investigate the thermodynamic of the hydrodesulfurization for the adsorbed thiophene on Au/ and Au_2/SAPO-11 we follow the mechanism proposed by Yao et al. [59] and Sullivan and Ekerdt [57]. The reaction enthalpy changes calculations were performed for the following reactions:

$$\text{Thiophene–Au/SAPO-11} + H_2 \rightarrow \text{2, 5-DHT–Au/SAPO-11} \quad (4)$$

$$\text{Thiophene–Au}_2\text{/SAPO-11} + H_2 \rightarrow \text{2, 5-DHT–Au}_2\text{/SAPO-11} \quad (5)$$

The calculated energy changes were $\Delta H = -23.0$ for reaction (4) and −36.8 kcal/mol, for reaction (5). The 2,5-DHT-Au/SAPO-11 structure is displayed in Fig. 5. Some other hydrogenation intermediates were calculated but 2,5-DHT always resulted to be the lower energy structure. The Au–S BI on thiophene–Au/SAPO-11 is 0.38 and 0.48 with 2,5-DHT. In the dimer case, one Au–S BI is 0.35 and the corresponding value on 2,5-DHT is 0.50. These values point out that the 2,5-DHT interaction is greater than the thiophene interaction with the Au/SAPO-11 catalyst. Further stepwise hydrogenation leads to the C–S scission, and then to the formation of 2-butene and H_2S, in both cases (Au and Au_2 with separated Au). The product of HDS of thiophene (2-butene) is displayed in Fig. 6, for both Au/SAPO-11 and Au_2/SAPO-11. The HDS reaction presents a $\Delta H = -50.0$ and −60.5 kcal/mol respectively.

The direct elimination of butadiene, from 2,5-DHT is obtained only with Au_2/SAPO-11 (see Fig. 7). This reaction has a $\Delta H = -17.5$ kcal/mol, and from the thiophene, it presents a $\Delta H = -54.3$ kcal/mol. This intramolecular elimination could not be attained with the Au/SAPO-11 model. This fact suggests that the mechanism is strongly dependent of the type of Au aggregate supported on SAPO-11. When S interacts with two Au, the direct elimination of butadiene could be achieved. Whereas, when there is only one Au, scission of one of the C–S bond is produced and the other C–S bond remains interacting with gold. In thiophene–Au_2/SAPO-11 (see Fig. 4b) the S–Au bond distances are 2.44 and 3.09 Å respectively and Au–Au bond distance (R) is 3.19 Å. This situation is similar in 2,5-DHT on Au_2/SAPO-11 in which the S–Au bond distances are 2.37 and 3.09 Å, and Au–Au R is 3.12 Å (see Fig. 5b). Thus, in the two precursor's molecular structures in the HDS, there is an interaction of one S with the two Au. This interaction could promote the direct intramolecular butadiene elimination (see Fig. 7), and this fact could explain that this mechanism is not reached with one single Au nor with the two Au atoms when S interacts only with one of the Au atom. HDS proceeds stepwise when S interacts with only one Au to obtain 2-butene (3 steps hydrogenation). On the contrary if S interacts with two Au atoms, then the direct intramolecular elimination of butadiene could occur (2 steps hydrogenation).

Recently, Suo et al. [67], have published an Au–Ni/SiO_2 bimetallic catalysts with high performance on HDS. The activity is affected by nickel and gold, as well as pre-treatment. It is found that the presence of gold partially reduce nickel sulfide phase, and significantly increases the HDS activity.

4. Conclusions

1. The Au/SAPO-11 and Au_2/SAPO-11 clusters are stable suggesting that their formations are amply probable on these type molecular structures.
2. The most stable conformations of thiophene adsorption on both Au/ and Au_2/SAPO-11 are η^1 type adsorption (trough the electron pair of S). This type of adsorption has a defined conformation with respect to the pore.
3. 2,5-DHT is obtained, by thiophene hydrogenation in both aggregates.
4. Thiophene HDS on Au/SAPO-11 produces 2-butene trough 2,5 intermediate, by step wise hydrogenation.
5. Thiophene HDS to 2-butene is also achieved on Au_2/SAPO-1.
6. Butadiene intramolecular direct elimination is attained on Au_2/SAPO-11 but exclusively when there is an interaction of S with the two Au atoms. This direct elimination is not obtained with the Au/SAPO-11 model. This fact indicates that the mechanism of reaction is highly dependent on the Au aggregate type supported on SAPO-11.
7. The simultaneous interaction of S with 2Au, could favor butadiene direct elimination on Au_2/SAPO-11.
8. The SAPO-11 could be of great interest as host material for dispersing Au.

References

[1] M. Haruta, T. Kobayashi, H. Sano, N. Yamada, Chem. Lett. (1987) 405.
[2] G.C. Bond, D.T. Thompson, Catal. Rev.-Sci. Eng. 41 (1999) 319.
[3] M. Haruta, Catal. Today 36 (1997) 153.
[4] Z. Qu, L. Giurgiu, E. Roduner, Chem. Commun. (2006) 2507.
[5] M. Mokhtar, I. Mekkawy, J. Phys. Chem. Solids 64 (2003) 299.
[6] A. Wang, J.H. Liu, S.D. Lin, T.S. Lin, J. Catal. 233 (2005) 186.
[7] G. Riach, D. Guillemot, M. Polisset, A.A. Khodadadi, J. Fraissard, Catal. Today 72 (2002) 115.
[8] S. Qiu, R. Ohnishi, M. Ichikawa, J. Phys. Chem. Lett. 98 (1994) 2719.
[9] T.M. Salama, R. Ohnishi, T. Shido, M. Ichikawa, J. Catal. 162 (1996) 169.
[10] X. Wang, A. Wang, X. Wang, T. Zhang, X. Yanga, React. Kinet. Catal. Lett. 92 (2007) 33.
[11] B.S. Uphade, T. Akita, T. Nakamura, M. Haruta, J. Catal. 209 (2002) 331.
[12] A.K. Sinha, S. Seelan, T. Akita, S. Tsubota, M. Haruta, Catal. Lett. (2003) 85.
[13] A.K. Sinha, S. Seelan, T. Akita, S. Tsubota, M. Haruta, Appl. Catal. A 240 (2003) 243.
[14] A.K. Sinha, S. Seelan, M. Okumura, T. Akita, S. Tsubota, M. Haruta, J. Phys. Chem. B 109 (2005) 3956.
[15] F. Salehirad, M.W. Anderson, J. Chem. Soc. Faraday Trans. 94 (1998) 2857.
[16] K.S. Yoo, J.-H. Kim, M.J. Park b, S.J. Kim, O.S. Joo, K.D. Jung, Appl. Catal. A 330 (2007) 57.
[17] C.M. López, L. Ramirez, V. Sazo, V. Escobar, Appl. Catal. A 340 (2008) 1.
[18] A.K. Sinha, S. Seelan, Appl. Catal. A 270 (2004) 245.

[19] P. Meriaudeau, V.A. Tuan, V.T. Nghiem, S.Y. Lai, L.H. Hung, C. Naccache, J. Catal. 169 (1997) 55.
[20] A.K. Sinha, S. Sivasanker, Catal. Today 49 (1999) 293.
[21] C.M. López, Y. Guillén, L. García, L. Gómez, A. Ramírez, Catal. Lett. 122 (2008) 267.
[22] S. Zhang, S. Li Chen, P. Dong, G. Yuan, K. Xu, Appl. Catal. A 332 (2007) 46.
[23] P. Liu, J. Ren, Y. Sun, Catal. Commun. 9 (2008) 1804.
[24] M. Hochtl, A. Jentys, H. Vinek, J. Catal. 190 (2000) 419.
[25] F. Machado, C.M. López, Y. Campos, A. Bolívar, S. Yunes, Appl. Catal. A 226 (2002) 241.
[26] A. Sierraalta, Y. Guillen, C.M. López, R. Martínez, F. Ruette, F. Machado, M. Rosa-Brussin, H. Soscún, J. Mol. Catal. A 242 (2005) 233.
[27] D.B. Akolekar, G. Foran, S.K. Bhargava, J. Synchrotron Rad. 11 (2004) 284.
[28] Gaussian 03, Revisión B04, Gaussian Inc., Pittsburg, PA, 2003.
[29] A. Sierraalta, R. Añez, E. Ehrmann, J. Mol. Catal. A 271 (2007) 185.
[30] X. Solans-Monfort, M. Sodupe, V. Branchadell, J. Sauer, R. Orlando, P. Ugliengo, J. Phys. Chem. B 109 (2005) 3539.
[31] J.T. Fermann, T. Moniz, O. Kiowski, T.J. McIntire, S.M. Auerbach, T. Vreven, M.J. Frisch, J. Chem. Theory Comput. 1 (2005) 1232.
[32] S. Namuangruk, P. Pantu, J. Limtraku, J. Catal. 225 (2004) 523.
[33] S. Namuangruk, D. Tantanak, J. Limtraku, J. Mol. Catal. A: Chem. 256 (2006) 113.
[34] J. Lomratsiri, M. Probost, J. Limtraku, J. Mol. Graphics Modell. 25 (2006) 219.
[35] N. Jiang, S. Yuan, J. Wuang, Z. Qin, H. Jiao, Y.-W. Li, J. Mol. Catal. A 232 (2005) 59.
[36] Z.-X. Gao, Q. Sun, H.-Y. Chen, X. Wang, W.M.H. Sachtler, Catal. Lett. 72 (2001) 1.
[37] M.M. Mohamed, T.M. Salama, R. Ohnishi, M. Ichikawa, Langmuir 17 (2001) 5678.
[38] M.M. Mohamed, T.M. Salama, M. Ichikawa, J. Colloid Inter. Sci. 224 (2000) 366.
[39] J.C. Fierro-Gonzalez, B.C. Gates, Chem. Soc. Rev. 37 (2008) 2127.
[40] I. Tuzovskaya, N. Bogdanchikova, A. Simakov, V. Gurin, A. Pestryakov, M. Avalos, M.H. Farıas, Chem. Phys. 338 (2007) 23.
[41] A. Simakov, I. Tuzovskaya, N. Bogdanchikova, A. Pestryakov, M. Avalos, M.H. Farias, E. Smolentseva, Catal. Commun. 9 (2008) 1277.
[42] N.N. Greenwood, A. Earnshow, Chemistry of the Elements, Pergamon, Oxford, 1984.
[43] A. Lachkar, A. Selmani, E. Sacher, M. Leclerc, R. Mokhliss, Synth. Met. 66 (1994) 209.
[44] F. Elfeninat, C. Fredriksson, E. Sacher, A. Selmani, J. Chem. Phys. 102 (1995) 6153.
[45] M. Honda, Y. Baba, N. Hirao, T. Sekiguchi, J. Phys.: Conf. Series 100 (2008) 052071.
[46] E. Ito, J. Noh, M. Hara, Surf. Sci. 602 (2008) 3291.
[47] S. Higai, J. Nara, T. Ohno, J. Chem. Phys. 121 (2004) 970.
[48] M.H. Dishner, J.C. Hemminger, F.J. Feher, Langmuir 12 (1996) 6176.
[49] T. Matsuura, M. Nakajima, Y. Shimoyama, Jpn. J. Appl. Phys. 40 (2001) 6945.
[50] J. Noh, E. Ito, K. Nakajima, J. Kim, H. Lee, M. Hara, J. Phys. Chem. B 106 (2002) 7139.
[51] J. Noh, E. Ito, T. Araki, M. Hara, Surf. Sci. 532–535 (2003) 1116.
[52] E. Ito, J. Noh, M. Hara, Jpn. J. Appl. Phys. 42 (2003) L852.
[53] E.O. Sako, H. Kondoh, I. Nakai, A. Nambu, T. Nakamura, T. Ohta, Chem. Phys. Lett. 413 (2005) 267.
[54] G. Liu, J.A. Rodriguez, J. Dvorak, J. Hrbek, T. Jirsak, Surf. Sci. 505 (2002) 295.
[55] A. Nambu, H. Kondoh, I. Nakai, K. Amemiya, T. Ohta, Surf. Sci. 530 (2003) 101.
[56] A.M. Venezia, V. La Parola, V. Nicol, G. Deganello, J. Catal. 212 (2002) 56.
[57] D.L. Sullivan, J.G. Ekerdt, J. Catal. 178 (1998) 226.
[58] J.A. Rodriguez, P. Liu, Y. Takahashi, K. Nakamura, F. Viñes, F. Illas, J. Am. Chem. Soc. 131 (2009) 8595.
[59] X.Q. Yao, Y.W. Li, H. Jiao, J. Molec. Struct.: THEOCHEM 726 (2005) 81.
[60] R. Prins, M. Egorova, A. Rothlisberger, Y. Zhao, N. Sivasankar, P. Kukula, Catal. Today 111 (2006) 84.
[61] X. Saintigny, R.A. van Santen, S. Clemendot, F. Hutschka, J. Catal. 183 (1999) 107.
[62] A.N. Startsev, J. Mol. Catal. A 152 (2000) 1.
[63] Y. Joshi, P. Ghosh, M. Daage, W.N. Delgass, J. Catal. 257 (2008) 71.
[64] B. Hinnemann, P.G. Moses, J. Nørskov, J. Phys.: Condens. Mat. 20 (2008) 1.
[65] P.G. Moses, B. Hinnemann, H. Topsøe, J. Nørskov, J. Catal. 248 (2007) 188.
[66] F. Besenbacher, M. Brorson, B.S. Clausen, S. Helveg, B. Hinnemann, J. Kibsgaard, J.V. Lauritsen, P.G. Moses, J.K. Nørskov, H. Topsøe, Catal. Today 130 (2008) 86.
[67] Z. Suo, A. Lv, H. Lv, M. Jin, T. He, Catal. Commun. 10 (2009) 1174.